

Some aspects of the fluid dynamics of laser welding

By JOHN DOWDEN,

Department of Mathematics, University of Essex, Colchester, U.K.

MICHAEL DAVIS AND PHIROZE KAPADIA

Department of Physics, University of Essex, Colchester, U.K.

(Received 5 November 1981)

When a laser beam is used as the energy source for welding two pieces of metal together, a hole is formed perpendicular to the plane of the workpiece. The latter is moved relative to the laser and metal is transferred from the front to the rear by fluid flow round the hole. The equations governing the process are set out and the conditions at the two boundaries in the problem (one between the hole and the molten metal, and the other between the liquid and the solid states of the metal) are considered.

Approximate solutions of the problem for low welding speeds are obtained for four different models. The first is one in which the viscosity is taken to be constant. In the second, the viscosity is allowed to depend linearly on temperature. The third model divides the liquid into a region in which the cooler part is taken to be viscous and the hotter part inviscid; the fourth model is then constructed as a limit, with the liquid motion considered as wholly inviscid. It is found that the motion is not irrotational in this last model. The models all display a downstream displacement of the boundary between the solid and liquid states, in agreement with observations. An expression for the minimum power of the laser is calculated.

1. Introduction

Lasers are being used in industry for an increasingly wide variety of purposes (La Rocca 1982); one purpose for which they are particularly well suited is to supply the energy for welding. A weld can be made with a laser beam that is pointed almost perpendicularly to the metal work-piece in the way shown in figure 1. Initially the beam creates a hole, but subsequently as the metal is moved relative to the laser this 'keyhole', as it is usually called, moves through the metal with only a small amount of matter lost by further vaporization. The power supplied by the laser beam leads to the melting of a region about the keyhole, whose cross-section is observed to be very close to circular, although its radius is not necessarily independent of depth (Klemens 1976). Metal then flows in this liquid region from the front of the hole to the rear, where it ultimately solidifies again. Some of the metal may cross the hole in the form of vapour, but this does not appear to be the main method of transfer.

The form of welding described above is rather similar to electron-beam welding and plasma-arc welding; a review of solved problems in heat conduction that can be used to model the effects of a laser is given by Duley (1976, chap. 4). The thermal aspects of the problem under consideration here have been studied in detail by Swift-Hook & Gick (1973), but they replaced the keyhole by a line source so that the metal moves relative to it with a constant velocity at all times. Holes of finite size have been

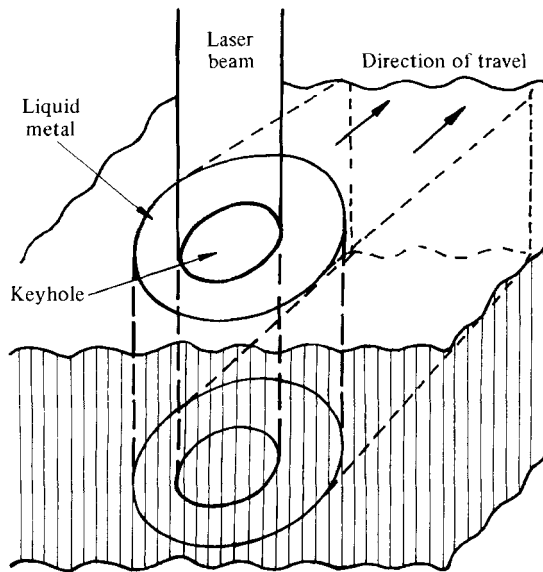


FIGURE 1. Geometry of laser beam relative to workpiece.

considered by Ol'shanskii (1974) for electron-beam welding and by Klemens (1976) for electron-beam and laser welding. The problem considered by Ol'shanskii did not involve complete penetration and included a substantial space behind the beam not directly influenced by it; the flow that resulted was driven by temperature variations in the surface tension, but that seems unlikely to be an important mechanism in our problem since the sides of the keyhole are necessarily at or near to boiling temperature, when the surface tension will be very small, but substantial transport of metal is still taking place. Klemens discusses the problem using approximate methods and obtains a self-consistent description of cavity formation and beam penetration but without detailed solutions for the pattern of flow and temperature distribution.

In this paper we shall investigate the steady continuous laser-welding process in which the metal translates with constant velocity U relative to a perpendicularly directed laser beam. We shall concentrate on the description of the flow of metal around the keyhole and of its temperature. For the purposes of obtaining analytical forms for the solution we shall make the two basic assumptions that the Péclet number of the flow is small, and that the motion is steady and two-dimensional. For two of the models discussed, the Prandtl number will be assumed to be of order unity, but the last two models include regions in which the fluid motion is inviscid.

The conditions on the liquid flow and temperature distribution at the boundary between the solid and liquid states are relatively straightforward; however, the conditions to be imposed on the surface separating the keyhole from the molten metal are less certain and require some consideration.

It is probable that the hole itself is kept open by a combination of the pressure of the plasma that forms in the keyhole and the recoil pressure of the evaporating metal, but conclusive information about this, either from experimental evidence or theoretical considerations, is not available. Another problem is that it does not seem

to be known for certain exactly how transfer of power from the laser beam takes place inside the keyhole. One possibility is that the power of the laser is absorbed and reflected directly at the surface of the metal, in a way that is well illustrated by Duley in the diagram on p. 246 of his book. It is quite possible that this is an important mechanism, but it does not seem entirely adequate. Experimental evidence shows that for pulsed laser beams falling on a metal surface an air plasma sometimes forms above the surface, and Pirri, Root & Wu (1978) have shown that the plasma substantially improves the coupling between the laser and the metal; energy transfer is then by reradiation from the plasma. In their example only pulsed lasers were considered, and in many ways the situation differs a good deal from that of penetration welding by a continuously working laser, but their work clearly shows how important the plasma can be. It seems that a plasma is formed in the keyhole; the laser passes some of its energy to the plasma, which then transmits it to the metal by a combination of reradiation and conduction. The rest of the energy is reflected by the plasma, absorbed directly by the metal or reflected before being absorbed.

In contrast to the approach of Pirri *et al.*, Mazumder & Steen (1980) use a model in which, as a device for calculation, points in the keyhole are treated as part of the metal, but at a fictitiously high temperature, and energy is allowed to pass from these into the liquid part of the metal by conduction. This is perhaps another extreme, but it is possible that lateral conduction is here as important as reradiation, since, in contrast to the situation considered by Pirri *et al.*, the process is taking place in a very confined space. In both of these explanations the existence of the plasma is crucial. If the density of the plasma is too great the energy is reflected and not absorbed, while in its absence welding does not take place, so there is clearly an optimum density. If the density is not uniform across the keyhole even the somewhat-deflected form of the hole with depth could be explained without appeal to direct absorption at the liquid surface.

It is usual to assist the welding process by blowing a stream of gas (helium or argon) coaxially with the laser beam; in the case of argon this also forms a plasma, which helps in the process of transfer of power, but in the case of helium there is no such interaction. One possible function of the jet may be to prevent the density of the metal plasma from becoming too great, since if it does the laser beam is reflected and welding ceases temporarily. There is therefore a steady (though quantitatively small) loss of metal by vaporization into the hole. The amount of matter lost may be small, but it plays an important part in the process and incidentally shows that the inner surface of the keyhole must be at or very close to the boiling point of the metal. We shall therefore assume that this surface is an isotherm with a temperature that will be taken as the boiling temperature; the heat transfer into the metal, though not important to the solution, can be related to the power of the laser, the radius of the keyhole, the speed of cutting, and the physical constants of the metal. Its relation to the power required from the laser means that it is a quantity of considerable practical interest, and it can be calculated after the solution has been obtained.

Conditions on the fluid motion are simpler: clearly there can be no tangential component of stress at the surface since the mixture of plasmas and gas in the keyhole cannot support one. The normal component, however, need not be constant, since the axial symmetry of the laser and the mechanics of the keyhole are such that to a first approximation the boundary also must have axial symmetry, stress perturbations associated with the metal flow being too small to have a significant effect.

It will be assumed that the variation in size of the hole with distance parallel to the beam is sufficiently small for it to have relatively little influence on the flow round the hole, so that the motion is effectively two-dimensional. In practice this will not always be the case, but in many instances the radial lengthscale of variation of temperature is in fact much less than the lengthscale parallel to the laser over which the keyhole changes diameter. It will be assumed that the amount of mass lost by vaporization is unimportant for this part of the calculation, even though, as mentioned above, it plays an important part in the thermodynamics of the process.

In practice all the physical constants of the material of the workpiece can be expected to depend on temperature; the specific heat of solid iron for example includes spikes and discontinuities in its temperature dependence (Austin 1932). We will, however, treat these properties as constants for the most part, or allow only differences between the solid and liquid states. No variations in density between solid and liquid states or with temperature in a given state will be considered.

There is one exception to the above remarks. The viscosity of a liquid normally depends heavily on temperature, and, although not much information on the variation of viscosity of liquid metals with temperature is available, there is no reason to suppose they are radically different in this respect. In particular we should expect the liquid to be substantially less viscous near its boiling point than near its freezing point, and that consequently its flow is likely to be more strongly concentrated near to the keyhole than would be predicted by a model in which the viscosity is constant. The first model studied in §3 (model I) is therefore one in which the viscosity is constant, and the second (model II) is one in which it is a linear function of temperature that vanishes at the boiling-point, but for which the Reynolds number of the flow as a whole is still low. The two models of §4 are an attempt to remove the small-Reynolds-number condition. The first (model III) is one in which the liquid region is divided into an outer layer in which the liquid is viscous and the Reynolds number small, and an inner layer that is treated as if the liquid were inviscid; one purpose of this model is to demonstrate the way in which the reduction of viscosity with temperature concentrates the flow near the keyhole. It has a second purpose, however; if the Prandtl number is taken to be small (for iron it is 0.057) it might sometimes be plausible to use an inviscid model for the liquid. In this case the continuity conditions at the interface between the solid and liquid phases are not entirely obvious, and so model III can be used to investigate what happens when a single inviscid layer is obtained by taking the limit of model III as the thickness of the viscous layer tends to zero. This limit is model IV, which models the liquid motion by that of an entirely inviscid fluid.

2. Governing equations and conditions at an interface

In a solid medium moving with a uniform velocity \mathbf{U} the equation governing the distribution of temperature T is

$$\frac{DT}{Dt} = \kappa_s \nabla^2 T, \quad (2.1)$$

where

$$\frac{D}{Dt} = \frac{\partial}{\partial t} + \mathbf{U} \cdot \nabla,$$

and κ_s is the thermal diffusivity of the solid corresponding to a thermal conductivity k_s (Batchelor 1967, p. 136) if the expansion of the material is ignored and k_s is assumed

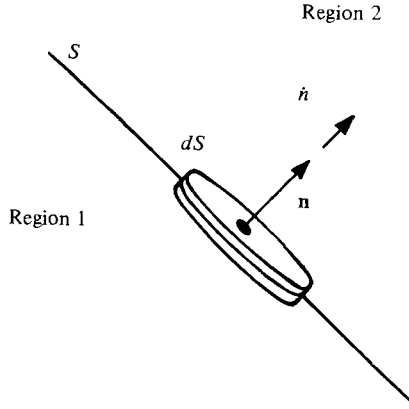


FIGURE 2. The normal \mathbf{n} relative to interface S between regions 1 and 2 showing conventions for positive directions; \dot{n} is the normal velocity of S in the direction of its own normal.

constant. The equations governing a fluid in motion are given by Batchelor (p. 164) as follows. The temperature equation is

$$\frac{DT}{Dt} = \kappa \nabla^2 T, \tag{2.2}$$

where

$$\frac{D}{Dt} = \frac{\partial}{\partial t} + \mathbf{u} \cdot \nabla,$$

provided that the expansion of the liquid is ignored, its density is taken to be constant and equal to that of the solid, and the conversion of mechanical into thermal energy is neglected; κ is the thermal diffusivity of the liquid and is related to ρ and the specific heat at constant pressure c_p , by

$$\kappa = \frac{k}{\rho c_p},$$

where k is the thermal conductivity, which has been assumed to be constant. The velocity vector is \mathbf{u} (with components $\{u_i\}$) at position $\mathbf{r} \equiv \{x_i\}$ and time t ; it then satisfies the equation of conservation of mass

$$\nabla \cdot \mathbf{u} = 0. \tag{2.3}$$

The Navier–Stokes equation is

$$\rho \frac{Du_i}{Dt} = \rho F_i - \frac{\partial p}{\partial x_i} + \frac{\partial}{\partial x_j} \left\{ \mu \left(\frac{\partial u_i}{\partial x_j} + \frac{\partial u_j}{\partial x_i} \right) \right\}, \tag{2.4}$$

if the applied body-force is \mathbf{F} ; μ is the coefficient of viscosity and p is the pressure.

Suppose that, at time t , S separates region 1 from region 2 and that it is described by the equation

$$S(\mathbf{r}, t) = 0;$$

let the unit normal from region 1 to region 2 be \mathbf{n} ; denote the velocity at which points on S move along \mathbf{n} by \dot{n} , and use subscripts 1 and 2 to distinguish between values of properties of the substance on either side of S (see figure 2). Then if $\nabla S \neq 0$

$$\mathbf{n} = \frac{\nabla S}{|\nabla S|}, \tag{2.5}$$

provided that the sign of S is chosen appropriately. From the definition of \dot{n}

$$S(\mathbf{r} + \dot{n}\mathbf{n} dt, t + dt) = S(\mathbf{r}, t) = 0;$$

subtracting these two equations, dividing by dt and taking the limit as $dt \rightarrow 0$ gives the result

$$\dot{n} = -\frac{\partial S/\partial t}{|\nabla S|}. \quad (2.6)$$

The rate at which mass crosses an almost-plane element of area dS of S from region 1 is

$$\rho_1(\mathbf{u}_1 \cdot \mathbf{n} - \dot{n}) dS,$$

which can be written as

$$\left[\rho \frac{DS}{Dt} \right]_1 dS/|\nabla S|$$

if use is made of (2.6), while the rate at which mass enters region 2 across it is similarly

$$\left[\rho \frac{DS}{Dt} \right]_2 dS/|\nabla S|.$$

Since conservation of mass requires these two to be equal, the limit as $dS \rightarrow 0$ gives the condition

$$\left[\rho \frac{DS}{Dt} \right]_1 = 0. \quad (2.7)$$

If the motion is steady and there is no change of density, this implies continuity of the normal component of velocity.

Conservation of thermal energy can be expressed in the same way (see e.g. Carslaw & Jaeger 1959, p. 284; Tayler 1975). The forms given by these authors may be modified to take account of the relative motion of the fluid phase by considering the rate at which heat flows towards S from region 1; this is $-k_1 \mathbf{n} \cdot \nabla T_1 dS$, while the rate at which it flows from the boundary into region 2 is $-k_2 \mathbf{n} \cdot \nabla T_2 dS$. The rate of release of heat on transition from 1 to 2 is $(\mathbf{u}_1 \cdot \mathbf{n} - \dot{n}) \rho_1 L_{12} dS$, where L_{12} is the latent heat of transition per unit mass: if 1 is liquid and 2 is solid, for example, it is the latent heat of melting. Conservation of thermal energy then requires that

$$-k_1 \mathbf{n} \cdot \nabla T_1 dS + (\mathbf{u}_1 \cdot \mathbf{n} - \dot{n}) \rho_1 L_{12} dS = -k_2 \mathbf{n} \cdot \nabla T_2 dS.$$

Use of (2.5) and (2.6) after division by dS and taking the limit as $dS \rightarrow 0$ shows that the condition can be written

$$[k\nabla T]_1^2 \cdot \nabla S + \rho \frac{DS}{Dt} L_{12} = 0. \quad (2.8)$$

There are further conditions on the velocity at such a transition. The force per unit area exerted by the substance in region 1 on that in region 2 is equal and opposite to the force exerted by 2 on 1. If both regions are fluid this condition becomes, in the absence of surface tension,

$$\left[-pn_i + \mu \left(\frac{\partial u_i}{\partial x_j} + \frac{\partial u_j}{\partial x_i} \right) n_j \right]_1^2 = 0$$

(Batchelor 1967, p. 150). The final condition that will be employed is that the tangential component of the velocity vector is continuous as the substance crosses S , so

$$[\mathbf{u}]_1^2 \times \mathbf{n} = 0. \quad (2.9)$$

At a change between a solid and a viscous fluid, or between two viscous fluid states, the reasons given by Batchelor (pp. 60, 149) apply. We shall assume that the condition also applies when the transition is between viscous and inviscid fluid states on the grounds that an impulsive accelerating force would be necessary otherwise, and the fluid possesses no mechanism for supplying such an impulse.

If the motion is two-dimensional, (2.3) can be satisfied exactly by introducing a stream function $\psi(x, y)$, where x, y are coordinates in the plane of motion and $\mathbf{u} = \nabla \times (\psi \mathbf{z})$ where \mathbf{z} is a unit vector perpendicular to the plane of motion.

If the motion of the fluid is considered to be inviscid, the body forces are ignored and the motion is steady, (2.4) can be solved to give

$$\nabla^2 \psi = f(\psi). \quad (2.10)$$

It will be seen later that the conditions of the problem require the equation to be linear, so that

$$\nabla^2 \psi = -\zeta \psi. \quad (2.11)$$

The pressure is then given by

$$p = p_0 + \frac{1}{2} \rho (\zeta \psi^2 - \nabla \psi^2). \quad (2.12)$$

Normally, the effects of viscosity must be taken into account, but we shall suppose that the velocity is sufficiently low for inertia forces to be neglected, as will be the case if

$$\rho a U \ll \mu, \quad (2.13)$$

where a is a characteristic length in the problem.

The stream function ψ is then a solution of

$$\mu \nabla^4 \psi + \nabla^2 (\nabla \mu \cdot \nabla \psi) + \nabla \mu \cdot \nabla \nabla^2 \psi - \nabla^2 \mu \nabla^2 \psi - \nabla \psi \cdot \nabla \nabla^2 \mu = 0, \quad (2.14)$$

which simplifies when μ is constant to

$$\nabla^4 \psi = 0. \quad (2.15)$$

Under these conditions, the pressure can be obtained by integrating

$$\nabla p = \mu \nabla \nabla^2 \psi \times \mathbf{z}. \quad (2.16)$$

The boundary conditions similarly simplify if all densities are taken to have the same value and the flow is steady; (2.7) and (2.9) then imply that the velocity is continuous across an interface, that is

$$[\mathbf{u}]_1^2 = \mathbf{0}. \quad (2.17)$$

The interface is an isotherm, and at it (2.8) shows that

$$([c_p \kappa \nabla T]_1^2 + L_{12} \mathbf{u}) \cdot \nabla S = 0. \quad (2.18)$$

3. Two single-layer models

In the models of this and §4 the evaporating boundary of the fluid is taken to be at $r = a$ (where polar coordinates (r, θ) are employed and $x = r \cos \theta$), with the basic assumption that the Péclet number is small, so that

$$Ua \ll \kappa_s, \kappa, \quad (3.1)$$

where κ_s and κ are the thermal diffusivities of the solid and the liquid respectively. In those models in which the effects of viscosity are included, the Prandtl number $\mu/\rho\kappa$ will be assumed to be of order unity. We shall then look for solutions in which

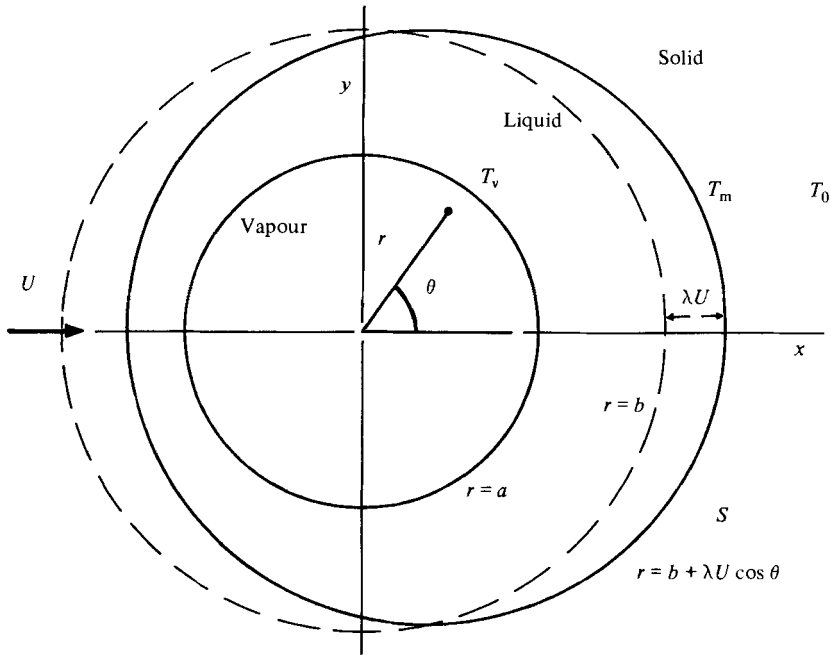


FIGURE 3. Cross-section of the keyhole and molten region for models I and II, showing the two interfaces.

the boundaries between the various regions are almost circular and which are consistent with an Oseen-type solution of the equation for the temperature, similar to that given by Lamb (1932, p. 615).

The first of the two models considered in this section is one in which the viscosity of the liquid metal is taken as constant, and the second is one where it is taken as a linear function of temperature which vanishes on the inner boundary. The general configuration is shown in figure 3. We shall find that it is possible to construct a solution in which the boundary between the solid and liquid states is at

$$r = b + \lambda U \cos \theta, \quad \text{i.e.} \quad S \equiv r - b - \lambda U \cos \theta; \tag{3.2}$$

the stream function in the liquid region is

$$\psi = Uf(r) \sin \theta; \tag{3.3}$$

the temperature in the liquid region is

$$T = g(r) + Uh(r) \cos \theta; \tag{3.4}$$

and the temperature in that part of the solid region for which r is not significantly greater than b is

$$T = l(r) + Um(r) \cos \theta. \tag{3.5}$$

Since (3.2) is an isotherm, $T = T_m$ (the melting temperature of the metal), linearization of the boundary conditions when applied to (3.5) shows that

$$l(b) = T_m, \quad \lambda l'(b) + m(b) = 0, \tag{3.6 a, b}$$

and in the same way

$$g(b) = T_m, \quad \lambda g'(b) + h(b) = 0. \tag{3.7 a, b}$$

The heat-flux condition (2.18) implies that

$$k_s l'(b) = kg'(b), \quad \rho L + k_s \{\lambda l''(b) + m'(b)\} - k \{\lambda g''(b) + h'(b)\} = 0, \quad (3.8a, b)$$

where k_s is the thermal conductivity of the solid state and k that of the liquid, and L is the latent heat of melting of the metal. The condition that $r = a$ is an isotherm on which T has the value T_v , the temperature at which the metal vaporizes, leads to the conditions

$$g(a) = T_v, \quad h(a) = 0. \quad (3.9a, b)$$

The conditions on the stream function ψ at $r = a$ are that it is the stream surface $\psi = 0$ and that the tangential component of the surface stress $e_{r\theta}$ vanishes.

In consequence

$$\lim_{r \rightarrow a^+} f(r) = 0, \quad (3.10)$$

$$\lim_{r \rightarrow a^+} \mu \{r f''(r) - f'(r)\} = 0. \quad (3.11)$$

At $r = b$ (2.17) requires that

$$f(b) = b, \quad f'(b) = 1. \quad (3.12a, b)$$

It is possible to find T in the solid region and the value of b by the method given by Lamb (1932, p. 615). For large value of r , T must satisfy (2.10) and thus have an asymptotic form

$$T \sim T_0 + C \exp\left\{\frac{Ur}{2\kappa_s}\right\} K_0\left(\frac{Ur}{2\kappa_s}\right)$$

(Carslaw & Jaeger 1959, p. 267), where T_0 is the temperature of the metal far away from the keyhole, C is a suitable constant and K_0 is a modified Bessel function. As $r \rightarrow \infty$ this tends to T_0 in all directions, and when r is small it has the approximate form

$$T_0 - C \left(\gamma + \ln \frac{Ur}{4\kappa_s} \right) - \frac{C}{2\kappa_s} \left(\gamma + \ln \frac{Ur}{4\kappa_s} \right) Ur \cos \theta$$

(γ is the Euler–Mascheroni constant), provided that

$$Ur \ll \kappa_s$$

but

$$\ln \frac{Ur}{4\kappa_s} = O(1).$$

Thus, provided that

$$b \sim a, \quad \ln \frac{Ua}{4\kappa_s} = O(1),$$

which can still be true even though (3.1) holds, the linearized form (3.5) of T , substituted in the linearized form of (2.1) and satisfying (3.6), must be

$$T = T_0 + \frac{T_m - T_0}{\gamma + \ln(Ub/4\kappa_s)} \left\{ \gamma + \ln \frac{Ur}{4\kappa_s} - \frac{U \cos \theta}{2\kappa_s} \left[\frac{b^2}{r} \ln \frac{Ub}{4\kappa_s} + \gamma \left(\frac{b^2}{r} - r \right) - r \ln \frac{Ur}{4\kappa_s} + \frac{2\lambda\kappa_s}{r} \right] \right\}. \quad (3.13)$$

In the liquid region g satisfies

$$g'' + \frac{1}{r} g' = 0,$$

and so (3.7a) and (3.9a) are satisfied if

$$g(r) = \frac{T_m \ln(r/a) - T_v \ln(r/b)}{\ln(b/a)}. \quad (3.14)$$

The condition (3.8a) then determines the value of the mean radius of the boundary between the solid and liquid states as

$$b = \frac{4\kappa_s}{U} \exp \left\{ \frac{k_s(T_m - T_0) \ln(aU/4\kappa_s) - \gamma k(T_v - T_m)}{k_s(T_m - T_0) + k(T_v - T_m)} \right\}. \quad (3.15)$$

So far the two models lead to identical results, although λ , which appears in (3.13), has yet to be determined. To find the fluid flow and that part of the temperature distribution in the liquid metal that depends on θ , the way in which the viscosity is allowed to vary with temperature must be taken into account. To calculate ψ to a linear approximation, only the term in μ independent of θ need be taken into account; and if in the second model μ is assumed to be given by

$$\mu = \mu_0 \frac{T_v - T}{T_v - T_m}$$

(giving $\mu = \mu_0$ on S and $\mu = 0$ on $r = a$) then it follows from (2.14) that $f(r)$ satisfies

$$\ln\left(\frac{r}{a}\right) \left(\frac{d^2}{dr^2} + \frac{1}{r} \frac{d}{dr} - \frac{1}{r^2} \right)^2 f + \left(\frac{d^2}{dr^2} + \frac{1}{r} \frac{d}{dr} - \frac{1}{r^2} \right) \frac{1}{r} \frac{df}{dr} + \frac{1}{r} \frac{d}{dr} \left(\frac{d^2}{dr^2} + \frac{1}{r} \frac{d}{dr} - \frac{1}{r^2} \right) f = 0. \quad (3.16)$$

In the first model, (2.15) implies that it satisfies

$$\left(\frac{d^2}{dr^2} + \frac{1}{r} \frac{d}{dr} - \frac{1}{r^2} \right)^2 f = 0. \quad (3.17)$$

It is possible to write the general solution of each of these equations in terms of four functions f_1, f_2, f_3 and f_4 , where $\{rf_i\}$ are solutions of (3.16) or (3.17) as appropriate, rf_1 and rf_2 satisfy both conditions (3.10) and (3.11), rf_3 satisfies (3.10) but not (3.11), and rf_4 satisfies (3.11) but not (3.10); expressions for them are given at the end of this section. The solution can therefore be expressed in terms of f_1 and f_2 only. In order to satisfy the two conditions (3.12a, b) it follows that

$$f(r) = \{\alpha_1 f_1(r) + \alpha_2 f_2(r)\} r, \quad (3.18)$$

where
$$\alpha_1 = \frac{f_2'(b)}{f_1(b)f_2'(b) - f_2(b)f_1'(b)} \quad \alpha_2 = -\frac{f_1'(b)}{f_1(b)f_2'(b) - f_2(b)f_1'(b)}$$

It is now possible to find $h(r)$. Suppose that the equation

$$\frac{d^2 h}{dr^2} + \frac{1}{r} \frac{dh}{dr} - \frac{h}{r^2} = \frac{1}{ar} f_i \quad (i = 1, 2)$$

has solutions
$$\frac{rh_1(r)}{a}, \quad \frac{rh_2(r)}{a},$$

where h_1 and h_2 both satisfy (3.9 b); once again, forms for these functions are given at the end of the section. Equation (2.2) implies that h is a solution of

$$\frac{d^2 h}{dr^2} + \frac{1}{r} \frac{dh}{dr} - \frac{h}{r^2} = \frac{f dg}{\kappa r dr} = \frac{T_m - T_v}{\kappa \ln(b/a)} \frac{f}{r^2}, \quad (3.19)$$

so h must be a suitable combination of rh_1, rh_2 and $a/r - r/a$. To satisfy (3.7b) it must be

$$h(r) = \frac{r(T_m - T_v)}{\kappa \ln(b/a)} \left\{ \left(\frac{\kappa \lambda}{b^2 - a^2} + \alpha_0 \right) \left(\frac{a^2}{r^2} - 1 \right) + \alpha_1 h_1(r) + \alpha_2 h_2(r) \right\}, \quad (3.20)$$

where

$$\alpha_0 = \frac{\alpha_1 h_1(b) + \alpha_2 h_2(b)}{1 - a^2/b^2}.$$

As a final stage it is now possible to satisfy (3.8b). This result is a condition that determines λ , whose value is found to be

$$\left[\rho L + \frac{k_s(T_m - T_0)}{\kappa_s(\gamma + \ln [Ub/4\kappa_s])} \left(\frac{1}{2} + \gamma + \ln \frac{Ub}{4\kappa_s} \right) \right] \frac{(b^2 - a^2) \ln(b/a)}{2k(T_v - T_m)} + \frac{b(b^2 - a^2)}{2\kappa} \left[\alpha_1 h_1'(b) + \alpha_2 h_2'(b) - \frac{2a^2\alpha_0}{b^3} \right]. \quad (3.21)$$

The functions f_i and h_i are given below.

For model I (in which the viscosity is constant)

$$\begin{aligned} f_1(r) &= \frac{a^2}{r^2} - \frac{r^2}{a^2}, & f_2(r) &= \ln \frac{r}{a}, \\ f_3(r) &= 1 - \frac{a^2}{r^2}, & f_4(r) &= 1 + \frac{a^2}{3r^2}, \\ f_1'(b) &= -2 \frac{a^4 + b^4}{a^2 b^3}, & f_2'(b) &= \frac{1}{b}; \\ h_1(r) &= -\frac{1}{2} \frac{a^2}{r^2} \ln \frac{r}{a} - \frac{1}{8} \left(\frac{r^2}{a^2} - 1 \right), \\ h_2(r) &= \frac{1}{4} \left(\ln \frac{r}{a} \right)^2 - \frac{1}{4} \ln \frac{r}{a}, \\ h_1'(b) &= \frac{a^2}{b^3} \ln \frac{b}{a} - \frac{a^2}{2b^3} - \frac{b}{4a^2} \\ h_2'(b) &= \frac{1}{2b} \ln \frac{b}{a} - \frac{1}{4b}. \end{aligned}$$

For model II, when the viscosity is allowed to depend linearly on T , the corresponding functions are

$$\begin{aligned} f_1(r) &= \int_{\xi=0}^{2 \ln(r/a)} I_0(\xi) d\xi, \\ f_2(r) &= \int_{\xi=0}^{2 \ln(r/a)} \mathbf{L}_0(\xi) d\xi, \\ f_3(r) &= \int_{\xi=0}^{2 \ln(r/a)} K_0(\xi) d\xi, \\ f_4(r) &= 1, \\ f_1'(b) &= \frac{2}{b} I_0 \left(2 \ln \frac{b}{a} \right), \\ f_2'(b) &= \frac{2}{b} \mathbf{L}_0 \left(2 \ln \frac{b}{a} \right); \\ h_1(r) &= \frac{1}{4} \left(2 \ln \frac{r}{a} - 1 \right) \int_0^{2 \ln(r/a)} I_0(\xi) d\xi + \frac{1}{2} \ln \left(\frac{r}{a} \right) \left\{ I_0 \left(2 \ln \frac{r}{a} \right) - 2I_1 \left(2 \ln \frac{r}{a} \right) \right\}, \\ h_2(r) &= \frac{1}{4} \left(2 \ln \frac{r}{a} - 1 \right) \int_0^{2 \ln(r/a)} \mathbf{L}_0(\xi) d\xi + \frac{1}{2} \ln \left(\frac{r}{a} \right) \left\{ \mathbf{L}_0 \left(2 \ln \frac{r}{a} \right) - 2\mathbf{L}_1 \left(2 \ln \frac{r}{a} \right) \right\} - \frac{1}{\pi} \ln \left(\frac{r}{a} \right), \end{aligned}$$

$$h_1'(b) = \frac{1}{2b} \int_0^{2 \ln(b/a)} I_0(\xi) d\xi + \frac{1}{b} \ln\left(\frac{b}{a}\right) \left\{ I_1\left(2 \ln \frac{b}{a}\right) - I_0\left(2 \ln \frac{b}{a}\right) \right\},$$

$$h_2'(b) = \frac{1}{2b} \int_0^{2 \ln(b/a)} L_0(\xi) d\xi + \frac{1}{b} \ln\left(\frac{b}{a}\right) \left\{ L_0\left(2 \ln \frac{b}{a}\right) - L_0\left(2 \ln \frac{b}{a}\right) \right\} + \frac{1}{\pi b} \left(2 \ln \frac{b}{a} - 1\right).$$

Here, I and K are modified Bessel functions, and L_0 and L_1 are modified Struve functions (see Abramowitz & Stegun 1965, p. 498). Note that the singularity of K_0 at $\xi = 0$ is integrable, so f_3 is well-defined.

4. The two-layer model

This model (model III) is the same as the constant-viscosity model of §3, except that there is a second layer adjacent to the keyhole in which viscosity is ignored in order to take partial account of the likelihood of almost inviscid flow in the region occupied by the hottest metal; if the Prandtl number of liquid metal at high temperatures is small it is possible for this to happen even though (3.1) holds. A relatively thin viscous layer immediately adjacent to the solid boundary may still occur. A similar notation to that used in §3 will be employed, except that quantities defined in the inviscid region will be distinguished by a bar placed over the top of the appropriate symbol; it should be noted that, in order to satisfy the discontinuity conditions, ψ must also have such a form in the inviscid region, and this is only possible if the unknown function in (2.10) is linear. In particular the boundary S between the viscous and inviscid region is given by

$$r = \bar{b} + \bar{\lambda} U \cos \theta, \quad (4.1)$$

and the temperature at which transition occurs by T . The general configuration is shown in figure 4. For simplicity we shall assume that the thermal conductivities and specific heats in the two fluid regions are the same, so that $\bar{\kappa} = \kappa$ and $\bar{k} = k$. In that case some of the results of §3 still apply; in particular the temperature in the solid region is still given in terms of λ by (3.13), the mean radius b of the solid/liquid boundary still has the value given in (3.15), while $g(r)$ and $\bar{g}(r)$ have the same analytical form given by (3.14). However, $g(b) = \bar{g}(\bar{b}) = \bar{T}$, so \bar{b} must be given by

$$\bar{b} = a \exp \left\{ \frac{(T_v - \bar{T}) \ln(b/a)}{T_v - T_m} \right\}. \quad (4.2)$$

Once again h satisfies (3.19), while \bar{h} is a solution of

$$\frac{d^2 \bar{h}}{dr^2} + \frac{1}{r} \frac{d\bar{h}}{dr} - \frac{\bar{h}}{r^2} = \frac{T_m - T_v}{\kappa \ln(b/a)} \frac{\bar{f}}{r^2}. \quad (4.3)$$

The forms for f and \bar{f} , however, are different. The function f satisfies (3.17) as before, but as a result of (2.11) \bar{f} is a solution of

$$\frac{d^2 \bar{f}}{dr^2} + \frac{1}{r} \frac{d\bar{f}}{dr} - \frac{\bar{f}}{r^2} = -\zeta \bar{f}; \quad (4.4)$$

ζ is a constant that relates the vorticity to the individual streamlines. There is no *a priori* reason to suppose that the flow in the inviscid region is irrotational.

The boundary conditions on f at \bar{S} , however, are that there is no stress (bearing

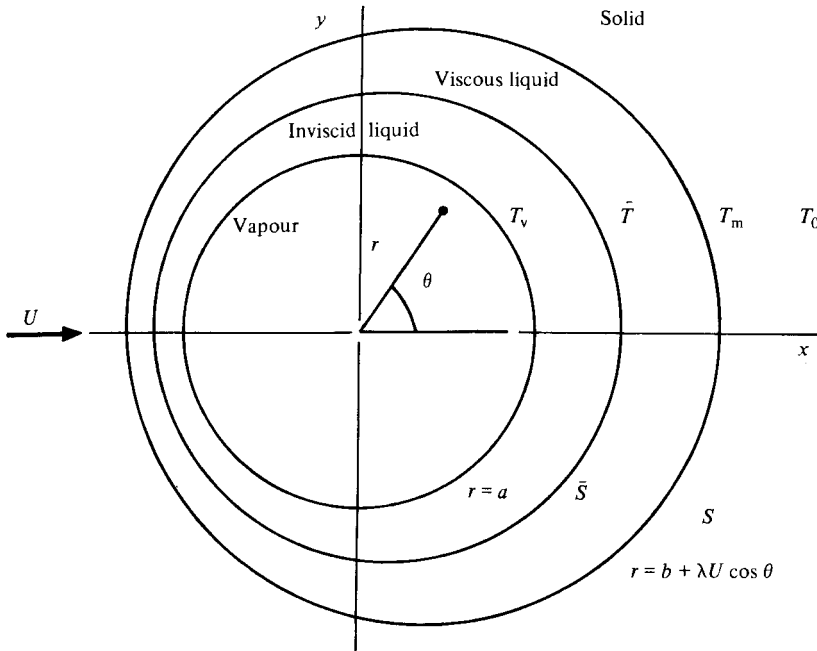


FIGURE 4. Cross-section of the keyhole and molten region for model III, showing the three interfaces.

in mind that the pressure in the inviscid region is, as (2.12) shows, necessarily of order $U^2\rho$ and therefore negligible in our model); so

$$f''(\bar{b}) - \frac{f'(\bar{b})}{\bar{b}} + \frac{f(\bar{b})}{\bar{b}^2} = 0, \tag{4.5}$$

and, since we now also require

$$p = p_0 + 2\mu \frac{\partial}{\partial r} \frac{1}{r} \frac{\partial \psi}{\partial \theta},$$

where p is given by (2.16), f must also satisfy

$$f'''(\bar{b}) + \frac{f''(\bar{b})}{\bar{b}} - \frac{4f'(\bar{b})}{\bar{b}^2} + \frac{4f(\bar{b})}{\bar{b}^3} = 0. \tag{4.6}$$

The only solution of (3.17) that satisfies all four conditions (3.12*a, b*), (4.5) and (4.6) is

$$f(r) = r. \tag{4.7}$$

In the inviscid region it is possible to write the stream function in terms of a single function \bar{f} that satisfies (4.4), $\bar{f}(a) = 0$ and $\bar{f}(\bar{b}) = f(\bar{b})$; its form is given at the end of this section. There is, however, an additional constraint imposed by (2.17). This requires that all components of \mathbf{u} , not just the normal one, should be continuous, and hence that $f'(\bar{b}) = \bar{f}'(\bar{b})$. Consequently

$$\frac{1}{2} \bar{b} \zeta^{\frac{1}{2}} [J_0(\bar{b} \zeta^{\frac{1}{2}}) Y_1(a \zeta^{\frac{1}{2}}) - Y_0(\bar{b} \zeta^{\frac{1}{2}}) J_1(a \zeta^{\frac{1}{2}})] = J_1(\bar{b} \zeta^{\frac{1}{2}}) Y_1(a \zeta^{\frac{1}{2}}) - Y_1(\bar{b} \zeta^{\frac{1}{2}}) J_1(a \zeta^{\frac{1}{2}}), \tag{4.8}$$

an equation that has to be solved numerically for the smallest positive value of ζ that satisfies it. All the expressions given above are in the form appropriate to a positive value of ζ ; they would apply equally well if it were negative, but investigation shows

that in fact there are no negative roots. It is readily checked that if $\zeta = 0$ no solution satisfying all three conditions on \bar{f} exists; it is interesting to note that (4.7) means that in fact there is steady uniform motion in the viscous part of the liquid, with all the transport around the keyhole taking place in the inviscid region.

It is now possible to find the temperature distribution. In the viscous region it is given by

$$T = g(r) + h(r) U \cos \theta,$$

where $g(r)$ is given in (3.14) and h satisfies (3.19) together with

$$h(b) + \lambda g'(b) = h(\bar{b}) + \bar{\lambda} g'(\bar{b}) = 0;$$

the form of h that satisfies these conditions is given at the end of this section. There is, however, an additional condition as a consequence of (2.18); it is the same as (3.8b) and leads to the condition

$$\bar{\lambda} - \lambda + \left\{ \rho L + \frac{k_s(T_m - T_0) \left(\frac{1}{2} + \gamma + \ln(Ub/4\kappa_s) \right) \right\} \frac{(b^2 - \bar{b}^2) \ln(b/a)}{2k(T_v - T_m)} + \frac{1}{4\kappa} \left\{ b^2 - \bar{b}^2 - 2\bar{b}^2 \ln \frac{b}{\bar{b}} \right\} = 0. \quad (4.9)$$

In this way a relation between λ and $\bar{\lambda}$ is obtained.

Finally the temperature distribution in the inviscid region can be found. It is of the form

$$T = g(r) + \bar{h}(r) U \cos \theta,$$

where $g(r)$ is given in (3.14) and \bar{h} is a solution of (4.3).

Since

$$\bar{h}(a) = 0, \quad \bar{\lambda} g'(\bar{b}) + \bar{h}(\bar{b}) = 0,$$

\bar{h} must have the form given at the end of this section. Lastly there is a condition that comes from (2.18) when $L_{12} = 0$ and $[c_p \kappa]_1^2 = 0$, which is so here since we are assuming that the thermal properties of the liquid are unchanged on transition from a viscous to an inviscid state.

The condition then implies that

$$h'(\bar{b}) = \bar{h}'(\bar{b}),$$

and so a second relation between λ and $\bar{\lambda}$ is obtained; it is

$$\lambda - \frac{\bar{\lambda}}{2} \left(1 + \frac{b^2}{\bar{b}^2} + \frac{(a^2 + \bar{b}^2)(b^2 - \bar{b}^2)}{\bar{b}^2(\bar{b}^2 - a^2)} \right) = \frac{1}{2\kappa} \left\{ \frac{1}{2}b^2 - \frac{1}{2}\bar{b}^2 - b^2 \ln \frac{b}{\bar{b}} + \bar{b}(b^2 - \bar{b}^2) \left[-\frac{a^2 + \bar{b}^2}{ab^2} \beta_0 + \beta_1 \bar{h}'_1(\bar{b}) + \beta_2 \bar{h}'_2(\bar{b}) \right] \right\}, \quad (4.10)$$

where \bar{h}_1 , \bar{h}_2 , β_0 , β_1 and β_2 are all defined below. Equations (4.9) and (4.10) can be solved for λ , $\bar{\lambda}$, and so the solution of the problem can in principle be obtained.

A case of special interest occurs when $\bar{T} = T_m$, so that the viscous layer is vanishingly thin. This is model IV, for which most of the expressions are the same as those obtained above, modified only by replacing b by \bar{b} and λ by $\bar{\lambda}$. However, (4.9) and (4.10) have to be solved for $\bar{\lambda}$ and a limit taken as $\bar{b} \rightarrow b$; this gives

$$\bar{\lambda} = \frac{(\bar{b}^2 - a^2) \ln(\bar{b}/a)}{2k(T_v - T_m)} \left\{ \rho L + \frac{k_s(T_m - T_0) \left(\frac{1}{2} + \gamma + \ln(U\bar{b}/4\kappa_s) \right) \right\} + \frac{\bar{b}^2 - a^2}{2\kappa} \left\{ \beta_0 \frac{a^2 + \bar{b}^2}{a\bar{b}} - \beta_1 \bar{b} \bar{h}'_1(\bar{b}) - \beta_2 \bar{b} \bar{h}'_2(\bar{b}) \right\}. \quad (4.11)$$

Functions and constants referred to above and used in the construction of the solution are as follows:

$$\bar{f}(r) = \bar{b} \frac{J_1(r\zeta^{\frac{1}{2}}) Y_1(a\zeta^{\frac{1}{2}}) - Y_1(r\zeta^{\frac{1}{2}}) J_1(a\zeta^{\frac{1}{2}})}{J_1(\bar{b}\zeta^{\frac{1}{2}}) Y_1(a\zeta^{\frac{1}{2}}) - Y_1(\bar{b}\zeta^{\frac{1}{2}}) J_1(a\zeta^{\frac{1}{2}})}, \quad (4.12)$$

$$h(r) = \frac{T_v - T_m}{2\kappa \ln(b/a)(b^2 - \bar{b}^2)} \left\{ rb^2 \ln\left(\frac{b}{r}\right) + r\bar{b}^2 \ln\left(\frac{r}{\bar{b}}\right) - \frac{b^2\bar{b}^2}{r} \ln\frac{b}{\bar{b}} + 2\kappa \left[\lambda \left(r - \frac{\bar{b}^2}{r} \right) - \bar{\lambda} \left(r - \frac{b^2}{r} \right) \right] \right\}, \quad (4.13)$$

$$\bar{h}(r) = \frac{\bar{b}(T_v - T_m)}{\kappa \ln(b/a)} \left\{ \left(\frac{a}{r} - \frac{r}{a} \right) \left(\beta_0 - \frac{\kappa\bar{\lambda}a}{b(\bar{b}^2 - a^2)} \right) + \beta_1 \bar{h}_1(r) + \beta_2 \bar{h}_2(r) \right\}, \quad (4.14)$$

where

$$\bar{h}_1(r) = \frac{1}{2r\zeta^{\frac{1}{2}}} \{ J_0(r_1\zeta^{\frac{1}{2}}) - J_0(a\zeta^{\frac{1}{2}}) \} + \frac{1}{2} r\zeta^{\frac{1}{2}} \int_{\xi=a\zeta^{\frac{1}{2}}}^{r\zeta^{\frac{1}{2}}} \frac{1}{\xi^2} J_1(\xi) d\xi,$$

$$\bar{h}_2(r) = \frac{1}{2r\zeta^{\frac{1}{2}}} \{ Y_0(r\zeta^{\frac{1}{2}}) - Y_0(a\zeta^{\frac{1}{2}}) \} + \frac{1}{2} r\zeta^{\frac{1}{2}} \int_{\xi=a\zeta^{\frac{1}{2}}}^{r\zeta^{\frac{1}{2}}} \frac{1}{\xi^2} Y_1(\xi) d\xi,$$

$$\beta_0 = \frac{a\bar{b}}{\bar{b}^2 - a^2} \{ \beta_1 \bar{h}_1(\bar{b}) + \beta_2 \bar{h}_2(\bar{b}) \},$$

$$\beta_1 = - \frac{Y_1(a\zeta^{\frac{1}{2}})}{\{ J_1(\bar{b}\zeta^{\frac{1}{2}}) Y_1(a\zeta^{\frac{1}{2}}) - Y_1(\bar{b}\zeta^{\frac{1}{2}}) J_1(a\zeta^{\frac{1}{2}}) \}},$$

$$\beta_2 = \frac{J_1(a\zeta^{\frac{1}{2}})}{\{ J_1(\bar{b}\zeta^{\frac{1}{2}}) Y_1(a\zeta^{\frac{1}{2}}) - Y_1(\bar{b}\zeta^{\frac{1}{2}}) J_1(a\zeta^{\frac{1}{2}}) \}},$$

$$\bar{h}'_1(\bar{b}) = \frac{1}{2\bar{b}^2\zeta^{\frac{1}{2}}} \{ J_0(a\zeta^{\frac{1}{2}}) - J_0(\bar{b}\zeta^{\frac{1}{2}}) \} + \frac{1}{2}\zeta^{\frac{1}{2}} \int_{\xi=a\zeta^{\frac{1}{2}}}^{\bar{b}\zeta^{\frac{1}{2}}} \frac{1}{\xi^2} J_1(\xi) d\xi,$$

$$\bar{h}'_2(\bar{b}) = \frac{1}{2\bar{b}^2\zeta^{\frac{1}{2}}} \{ Y_0(a\zeta^{\frac{1}{2}}) - Y_0(\bar{b}\zeta^{\frac{1}{2}}) \} + \frac{1}{2}\zeta^{\frac{1}{2}} \int_{\xi=a\zeta^{\frac{1}{2}}}^{\bar{b}\zeta^{\frac{1}{2}}} \frac{1}{\xi^2} Y_1(\xi) d\xi.$$

5. Comparison of the models

Results for each of the four models have been worked out taking the following values (appropriate for iron) for the various parameters of the problem:

$$T_v = 2726.84 \text{ }^\circ\text{C}, \quad T_m = 1371.12 \text{ }^\circ\text{C}, \quad T_0 = 20 \text{ }^\circ\text{C}, \quad L = 266.7 \text{ J g}^{-1},$$

$$\rho = 7.2 \text{ g cm}^{-3},$$

$$k_s = 0.694 \text{ J cm}^{-1} \text{ s}^{-1} \text{ }^\circ\text{C}^{-1}, \quad \kappa_s = 0.213 \text{ cm}^2 \text{ s}^{-1}, \quad k = 0.327 \text{ J cm}^{-1} \text{ s}^{-1} \text{ }^\circ\text{C}^{-1},$$

$$\kappa = 0.0551 \text{ cm}^2 \text{ s}^{-1}$$

The welding speed and radius of the keyhole were taken to be $U = 0.75 \text{ cm s}^{-1}$, $a = 0.015 \text{ cm}$ (data supplied by the Welding Institute; for the size of hole that may be produced see also La Rocca 1982; Andrews & Atthey 1976).

For model III, \bar{T} has been taken as the mean of T_m and T_v . The condition (3.1) is only marginally satisfied; these values are at the lower end of the range used in practice and lead to solutions that satisfy the boundary conditions reasonably well. The least-satisfactory aspect of this choice is that the Reynolds number is not as small as could be wished. The value of b , the mean radius of the boundary between the liquid and solid states, is the same in all four models. For comparison, the value of this and other constants of the solutions are given in table 1; $a\zeta^{\frac{1}{2}}$ is given as well as ζ since

	Model I	Model II	Model III	Model IV
b (cm)	0.0500	0.0500	0.0500	—
\bar{b} (cm)	—	—	0.0274	0.0500
λ (s)	0.0235	0.0239	0.0246	—
$\bar{\lambda}$ (s)	—	—	0.00776	0.0241
ζ (cm ⁻²)	—	—	7230	362
$a\zeta^{\frac{1}{2}}$	—	—	1.28	0.286
§3	3, 4, 13, 14, 15, 18, 20, 21	3, 4, 13, 14, 15, 18, 20, 21	4, 13, 14, 15	13, 14, 15
§4	—	—	2, 8, 9, 10, 12, 13, 14	8, 11, 12, 14

TABLE 1. Constants of the solutions for each model, and references to equations describing the solutions

the former is a dimensionless number, but it should be remembered that it depends on all the other constants of the problem. Reference to equations in §§3 and 4 above that describe the solution for each model are also included in the table.

All the models have a number of qualitative features in common, and, in order to display these, model I will be described in some detail. Figure 5 shows the temperature distribution, with the temperature in the liquid shown in (a) and in the solid on a much smaller scale in (b). In the liquid there is a rise in temperature that is very nearly axisymmetric: the departures are not obvious in this projection. The asymmetry of the distribution in the solid however is quite clear, with high temperatures reaching further behind the laser than they do in front.

Figure 6(a) shows a graph of the stream function ψ in the liquid, and a contour map of it is shown in figure 6(b). As is to be expected, these show that the metal flows round the hole with a velocity that is greatest in the plane containing the laser beam and perpendicular to the direction of motion. A contour map of the radial component of velocity is shown in figure 7(a) and of the azimuthal component in figure 7(b). The latter shows that the velocity of flow is greatest in the plane $\theta = \frac{1}{2}\pi$ somewhere near the middle of the liquid region, and not at the free boundary.

The two main ways in which the models differ from each other are in the character of the fluid flow, and in the nature of departures from the axisymmetric temperature distribution. The first are most clearly seen by comparing graphs of $f'(r)$ for each of the models (equivalent to comparing the magnitudes of the velocities at $\theta = \frac{1}{2}\pi$), and graphs of $h(r)$. The former are shown in figure 8 and the latter in figure 9.

The velocity profiles shown in figure 8 illustrate the way in which there is a progressive relaxation of the influence of the conditions on the surface stress at $r = a$ as we move from model I to model II and then model IV. The fluid transport becomes more and more concentrated near to the keyhole, with consequences that will be seen when h is considered. The graph of model III appears almost like two straight-line segments; in fact the portion in $a < r < \bar{b}$ is not quite straight but is so to a fairly good approximation with this particular choice of parameters. The continuity and stress conditions require uniform motion in $\bar{b} < r < b$, so that the departure in the inviscid region of flow is necessarily greater.

It will be seen from figure 9 that the downstream displacement of the isotherms, indicated in detail by h and in outline by the values of λ and $\bar{\lambda}$ given in table 1, are in fact very similar for models I, II and IV. This is an accidental consequence of the

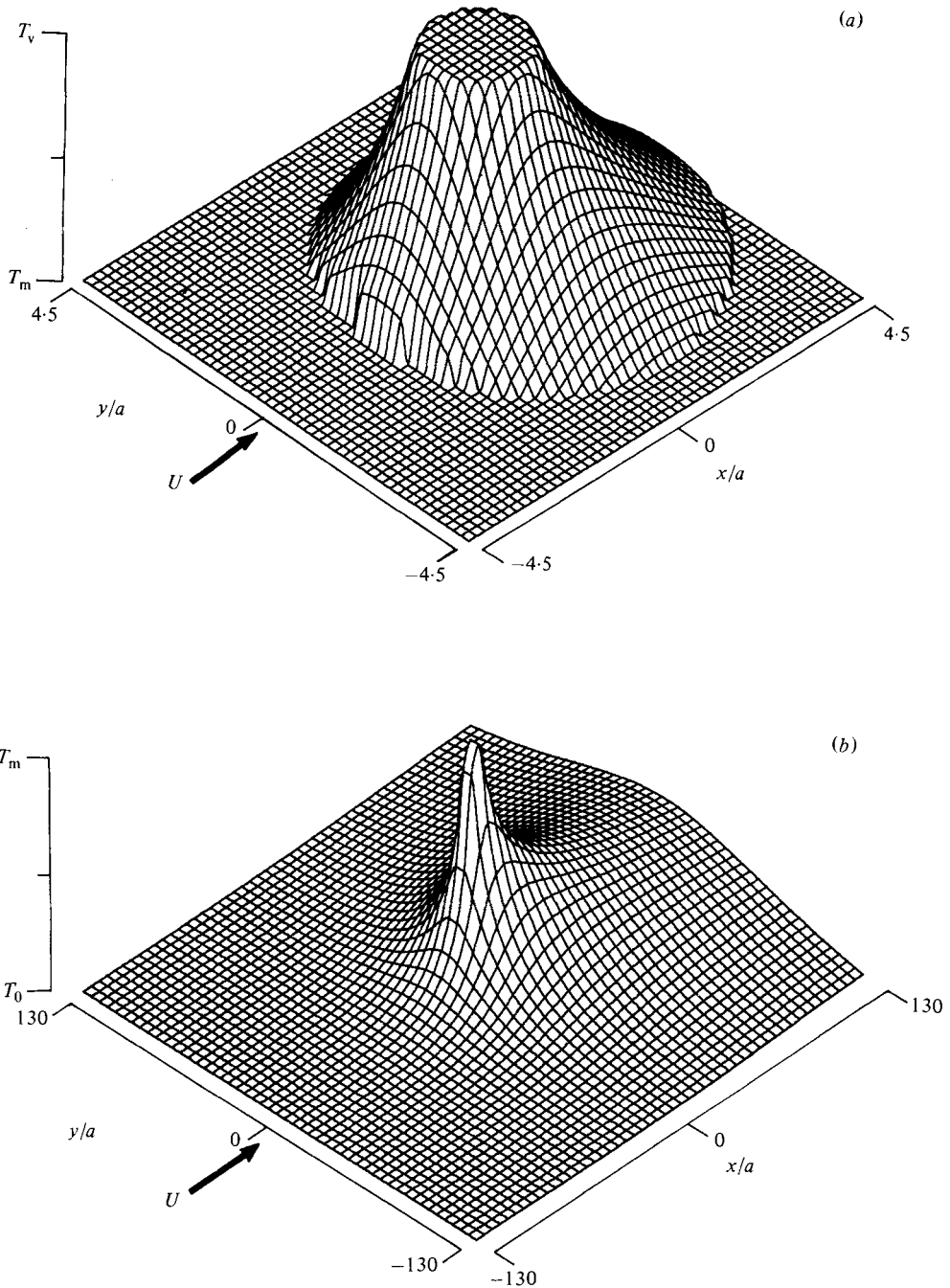


FIGURE 5. (a) Temperature in the liquid region for model I; for clarity T has been given the value of T_v inside the keyhole and T_m in the solid region. (b) Temperature in the solid region, to a much smaller scale.

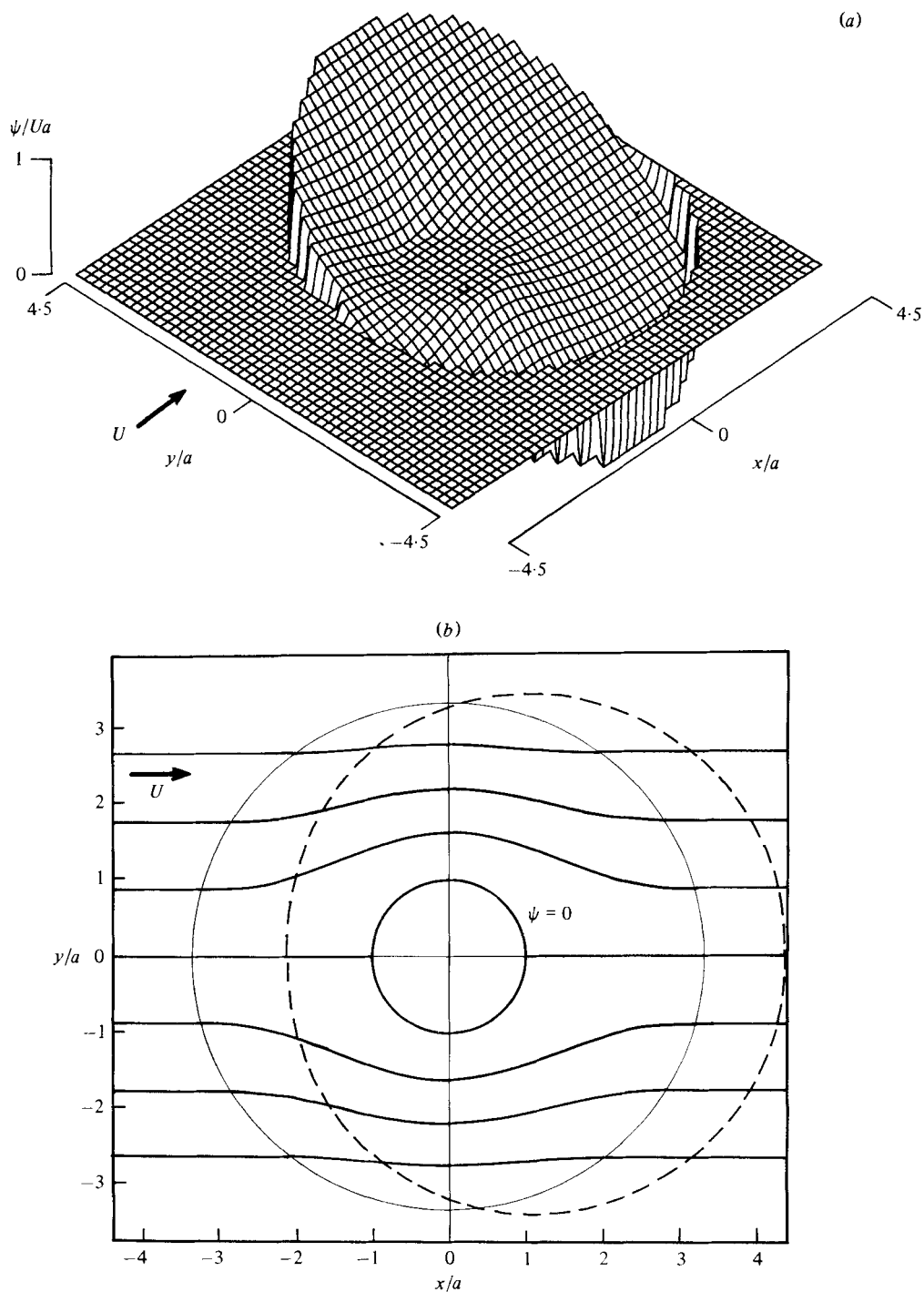


FIGURE 6. The stream function for model I. (a) Graph; for clarity it has been given a value of zero outside the liquid region. (b) Contour map; contours at multiples of $0.01 \text{ cm}^2 \text{ s}^{-1}$. The two circles show $r = a$ and $r = b$, between which f is defined. The broken curve shows the next approximation to the location of the outer boundary.

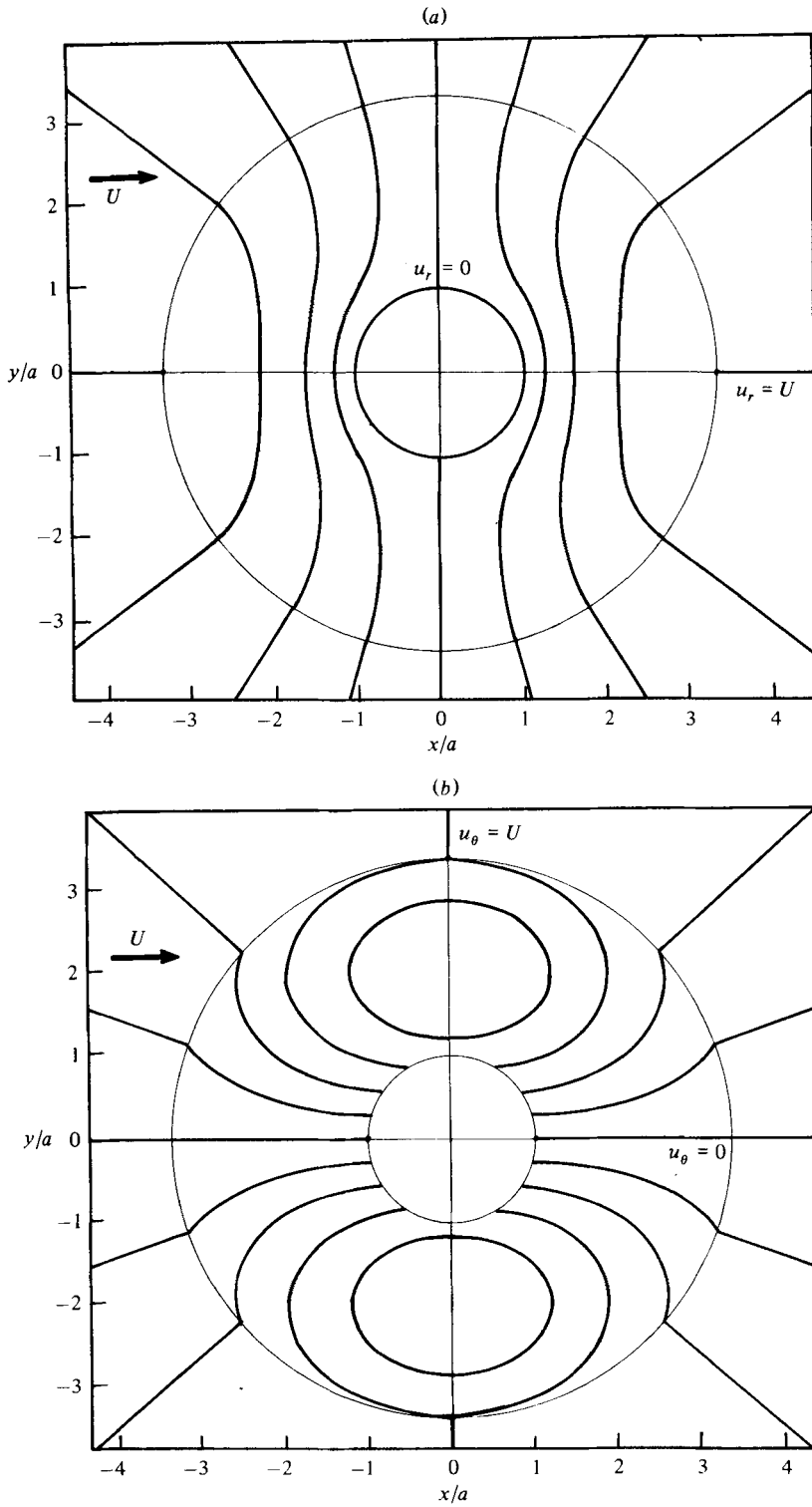


FIGURE 7. Contour maps of the velocity components for model I. (a) Radial component; contours at multiples of 0.2 cm s^{-1} . (b) Azimuthal component; contours at multiples of 0.25 cm s^{-1} .

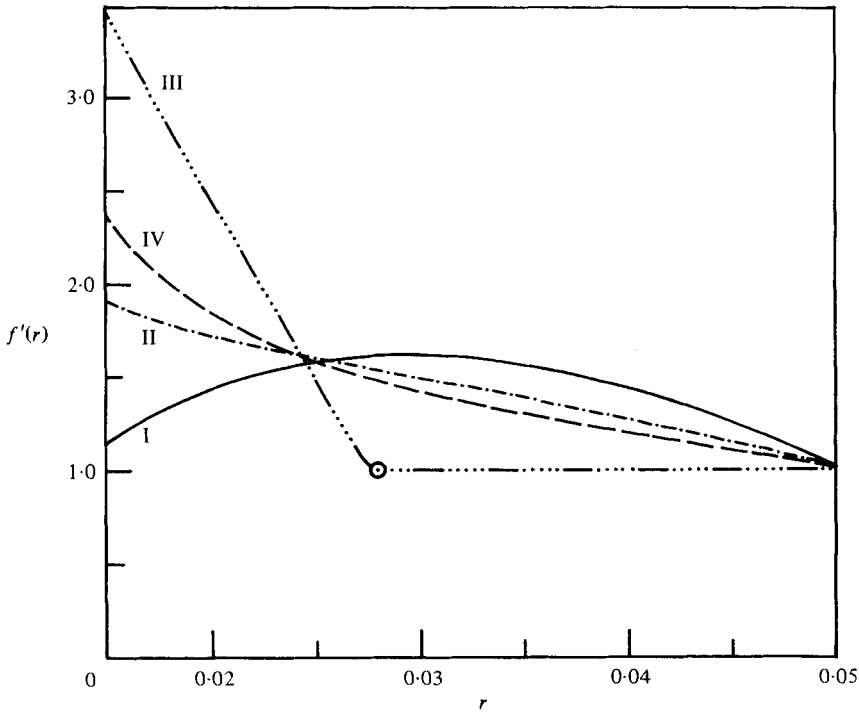


FIGURE 8. Graph of $f'(r)$, equal to $-u_\theta/U$ at $\theta = \frac{1}{2}\pi$, for each of four models in the liquid region: —, model I; - · - · - ·, model II; · · · · ·, model III; — — —, model IV. The circle on the curve for model III is drawn at $r = \bar{b}$ to show the point of transition between the viscous and inviscid states.

particular choice of material constants; the forms for $\alpha_0 - \alpha_2$ and $\beta_0 - \beta_2$ tend to magnify the fact that κ_s is fairly large compared with κ , so that h in (3.20) and \bar{h} in (4.14) are both quite well approximated by ignoring the terms in α and β . Similar remarks apply to λ and $\bar{\lambda}$. The form of the isotherms is rather different in model III, where most of the departure of the fluid motion from uniform flow occurs much nearer to the keyhole. The result is that heat is convected more strongly downstream from the keyhole than in the other models. To a lesser extent models II and IV show the same feature when compared with model I (see the values of λ ; the difference is too small to show clearly in figure 9). It is probable that the reason for the difference is that, in cases where most of the motion occurs near to the keyhole, the velocities are higher, giving less time for lateral diffusion of heat from the laser. The temperature distribution found here agrees well with that obtained by Mazumder & Steen (1980), and is similar to that found by Malmuth (1976).

A quantity of practical interest is the rate of supply of energy. This is given per unit length of the keyhole by

$$-\int_{\theta=0}^{2\pi} ak \left. \frac{\partial T}{\partial r} \right|_{r=a} d\theta, \quad (5.1)$$

where T is the temperature in the molten metal. Working to the linear approximation employed here we find that it is equal to

$$-2\pi ak g'(a),$$

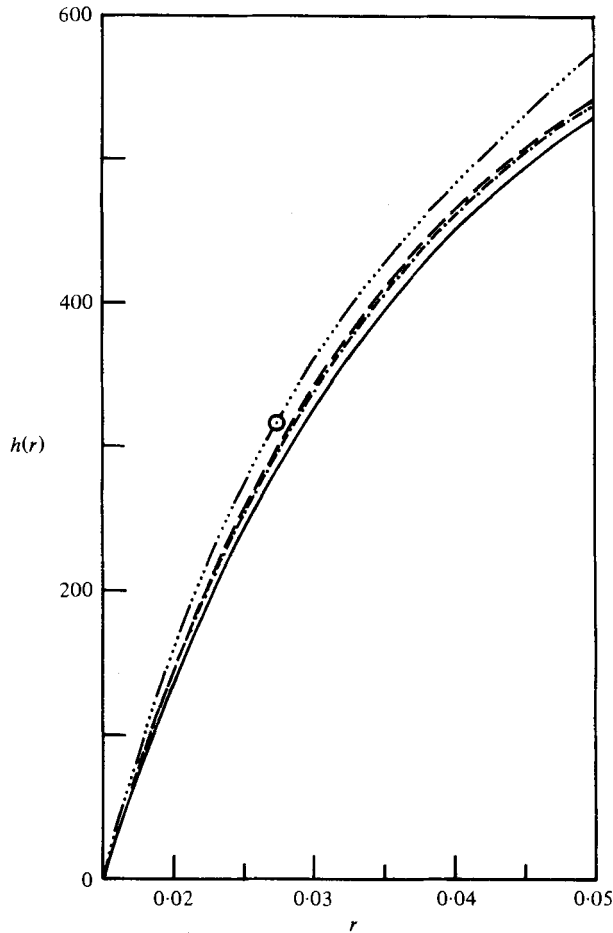


FIGURE 9. Graph of $h(r)$, proportional to that part of the temperature field which depends on θ , for each model in the liquid region. The curves are distinguished by the same conventions as for figure 8.

where g is given by (3.14) and is the same for all four models. It is therefore

$$-2\pi \frac{k_s(T_m - T_0) + k(T_v - T_m)}{\gamma + \ln(aU/R\kappa_s)}, \tag{5.2}$$

with a numerical value for the case given in this section of 2314 W cm^{-1} . Notice, however, that in steel, for example, the ratio of latent heat of evaporation to the heat required to raise the metal to its boiling point is large (Andrews & Atthey 1975), so that, even though the total mass of metal vaporized without recondensation in the keyhole may be small as indicated in §1, the amount of heat required for this purpose may not necessarily be negligible. Equation (5.2) does not include it, nor does it include heat lost by reflection or radiation from the ends of the keyhole, or convected away in the form of hot gas. Nor does it take account of yet further heating of the lost metal vapour beyond its boiling point. It is not possible to find the way in which the different models affect the heat flux given by (5.1) without solving (partially, at least) for the terms of order U^2 ; however, (5.2) shows that, to the approximation considered here, an increase in the speed of welding requires an increase in the rate

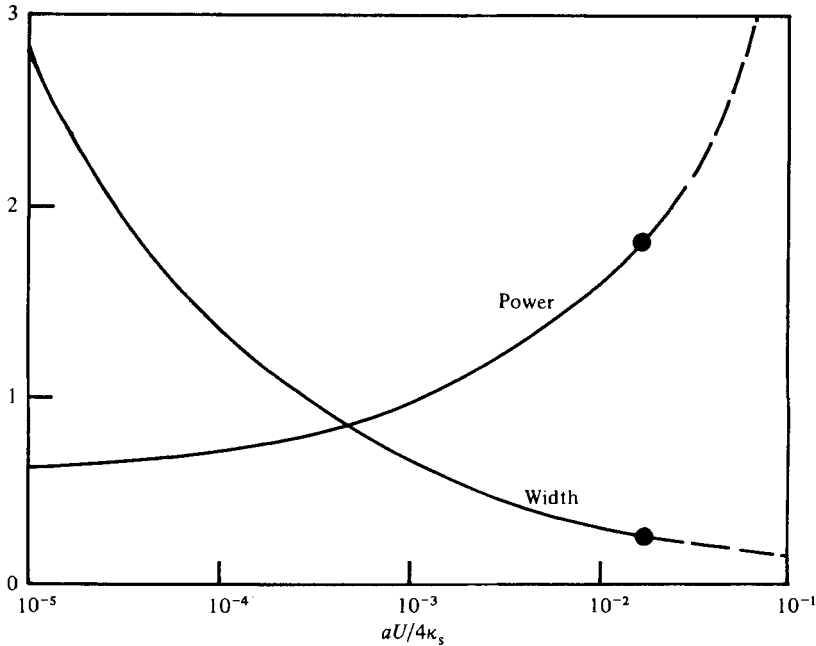


FIGURE 10. Graph of power W consumed per centimetre as a function of $aU/4\kappa_s$ for stationary keyhole conditions; the function $W/\{k_s(T_m - T_0) + k(T_v - T_m)\}$ is given. Also shown is $b/12a$, a measure of the width of the weld, with $c = 0.679$. The solid circles show points on the curves corresponding to the values of the parameters in the case studied here.

of supply of thermal energy, on the assumption that the keyhole size is unaltered. Similarly, the thermal power required increases with keyhole size; to use as little power as possible the product aU should be kept as small as possible. The power consumption is of practical importance, so its relation to aU is shown in figure 10 for a range of values consistent with the approximations used here. The width of the weld itself is also of some interest and is equal to $2b$, where b is given by (3.15); this is equivalent to a power-law dependence on both the radius a of the keyhole and the welding speed U . In dimensional form it can be written

$$b = a^c U^{-1+c} (4\kappa_s e^{-\gamma})^{1-c},$$

where

$$c = \left\{ 1 + \frac{k(T_v - T_m)}{k_s(T_m - T_0)} \right\}^{-1}.$$

This relationship is also shown in figure 10, plotted in dimensionless form with a value for c appropriate to the constants used here.

It is of some interest to notice that in model IV ζ is not zero, so that the inviscid molten metal is not in irrotational motion. The important feature here is that the velocity is continuous in the transition from the solid to the inviscid liquid, so the boundary conditions cannot in general be satisfied by an irrotational flow. It should be noted that the solid and liquid regions are different phases of the same material, with the consequence that the boundary between them is not sharply defined. There will be a region in which both solid and liquid phases exist together in thermodynamic equilibrium, with a thickness of the order of 10^{-5} m (Andrews, Atthey & Byatt-Smith 1980). The effects of viscosity acting at very short lengthscale can therefore generate vorticity in the same way that it may be generated at a porous boundary. It is likely

that the result obtained here hides a basic asymmetry between the melting and freezing processes. It seems natural that the tangential component of velocity should be continuous as the metal melts, since if it were not, the substance would have to be accelerated impulsively, and a fluid would not be capable of applying such a force. On freezing, however, the molten metal is 'captured' by the solid substance, and it is quite possible for it to be impulsively decelerated to match the tangential velocity of the solid. The fact that the vorticity is not zero here could mean that caution is necessary in models of related processes. Andrews & Atthey (1976) for example assume that the flow of liquid in the ablating surface of a laser-produced cavity is irrotational; the geometry and assumptions of their problem are rather different, so the approximation may be justifiable, but it cannot be regarded as obvious.

Values for the parameters of the model appropriate to a number of other metals have been used and the corresponding forms of the solutions obtained. All give qualitatively similar results, with the least variations from uniform flow being given (in all cases) by the variable-viscosity example (model II); the model with the highest velocity on the vaporizing boundary was always model IV. The differences between the models in the effect of convection on the temperature distribution was greater in metals with a low thermal conductivity such as lead than in, for example, aluminium with a high thermal conductivity. In all cases model I gave the least effect and model IV the greatest, with model II lying between them.

We have seen that it is possible to obtain approximate solutions for the liquid flow of molten metal past the keyhole formed during laser welding at low speeds. The conditions for validity of the models are (3.1) in all cases, and (2.13) in models I, II and in the outer molten region of model III. The models reproduce the observed downstream displacement of the boundary between the solid and liquid states, and this feature is found to be more marked in those models for which the fluid motion is concentrated nearer to the keyhole.

One of us (M. Davis) is indebted to the Welding Institute and the Science and Engineering Research Council for the award of a Case Studentship.

REFERENCES

- ABRAMOWITZ, M. & STEGUN, I. A. 1965 *Handbook of Mathematical Functions*. Dover.
- ANDREWS, J. G. & ATTHEY, D. R. 1975 On the motion of an intensely heated evaporating boundary. *J. Inst. Maths. Applics* **15**, 59–72.
- ANDREWS, J. G. & ATTHEY, D. R. 1976 Hydrodynamic limit to penetration of a material by a high-power beam. *J. Phys. D: Appl. Phys.* **9**, 2181–2194.
- ANDREWS, J. G., ATTHEY, D. R. & BYATT-SMITH, J. G. 1980 Weld-pool sag. *J. Fluid Mech.* **100**, 785–800.
- AUSTIN, J. B. 1932 Heat capacity of iron. *Indust. Engng Chem.* **24**, 1225–1235.
- BATCHELOR, G. K. 1967 *An Introduction to Fluid Dynamics*. Cambridge University Press.
- CARSLAW, H. C. & JAEGAR, J. C. 1959 *Conduction of heat in solids*. Clarendon.
- DULEY, W. W. 1976 *CO₂ Lasers: Effects and Applications*. Academic.
- KLEMENS, P. G. 1976 Heat balance and flow conditions for electron beam and laser welding. *J. Appl. Phys.* **47**, 2165–2174.
- LAMB, H. 1932 *Hydrodynamics*, 6th edn. Cambridge University Press.
- LA ROCCA, A. V. 1982 Laser applications in manufacturing. *Sci. Am.* **246**(3), 80–87.
- MALMUTH, N. D. 1976 Temperature field of a moving point-source with change of state. *Int. J. Heat Mass Transfer* **19**, 349–354.

- MAZUMDER, J. & STEEN, W. M. 1980 Heat transfer for cw laser material processing. *J. Appl. Phys.* **51**, 941–947.
- OL'SHANSKII, N. A. 1974 Movement of molten metal during electron-beam welding. *Svar. Proiz.* **9**, 12–14.
- PIRRI, A. N., ROOT, R. G. & WU, P. K. S. 1978 Plasma energy transfer to metal surfaces irradiated by pulsed lasers. *A.I.A.A. J.* **16**, 1296–1304.
- SWIFT-HOOK, D. T. & GICK, A. E. F. 1973 Penetration welding with lasers. *Welding J.* **52**, 492s–499s.
- TAYLER, A. B. 1975 The mathematical formulation of Stefan problems. In *Moving boundary problems in heat flow and diffusion* (ed. J. R. Ockendon & W. R. Hodgkin), pp. 120–137. Clarendon.